Oral Radiology (2020) 36:1–17
https://doi.org/10.1007/s11282-019-00367-4

REVIEW ARTICLE

The most frequent and/or important lesions that affect the face and the jaws

David MacDonald[1,2]

Received: 20 December 2018 / Accepted: 7 January 2019 / Published online: 13 February 2019

Abstract

Introduction The radiology of the most important and/or frequent lesions affecting the bones of the face and jaws has been set out in this review and pictorial essay.

Methods The latter is composed of multiple images displaying one or more key radiological features derived from almost every one of the most important and/ or frequent lesion affecting the face and the jaws. These images have been grouped together in 18 figures, each served by a detailed and free-standing legend. These lesions are outlined in a flowchart, which focuses on one or at most two radiological features in turn.

Results It begins with those lesions that could indicate systemic disease, such as multiple lesions, and then proceeds onward to single lesions. The first of these single lesions are the neoplasms which need not only an early diagnosis, but also complete ablation in the majority of cases. Cystic lesions are then next, including consideration of the frequently occurring non-cysts such as simple bone cysts and lingual bone defects which require no treatment. Finally, it ends with the periapical radiolucency of inflammatory origin.

Conclusion The most important and/or frequent lesions affecting the bones of the face and jaws that present to the oral and maxillofacial clinician can be considered systematically en route to the 'periapical radiolucency of inflammatory origin,' which is one of the most usually encountered lesions in clinical dentistry.

Keywords Radiology · Computed tomography · Cone-beam computed tomography · Fibro-osseous lesions · Face · Jaws

Introduction

It is the purpose of this paper to review the radiological presentation of the most frequent and/or important lesions affecting the bones of the face and the jaws. These are set out in Fig. 1. The calcified carotid artery atheroma and its differential diagnosis of radiopacities presenting in the soft tissues of the neck have been already fully addressed elsewhere [1]. Although a three-dimensional (3D) perception of the anatomy and lesion by conventional radiography (CR) is limited, the vast majority of lesions are diagnosed by CR alone. CR is also superior to any advanced imaging modality due to its ease of access, low-cost, relatively very low radiation dose, and superior spatial resolution. Furthermore, the conventional panoramic radiograph will display the entire jaws optimally exhibiting the site and extent of lesions, such as that of systemic sclerosis (scleroderma) in Fig. 2a [2]. Since CR of the most important and/or frequent lesions affecting the face and jaws has been fully addressed in the standard radiology textbooks, the limited space in this paper will be dedicated to cross-sectional imaging, substantially derived from cone-beam computed tomography (CBCT). These will reveal a perspective of these lesions hitherto not obvious on two-dimensional (2D) CR images alone. CBCT also enhances pre-surgical planning of cysts and benign neoplasms of up to four dental units [3]. Lesions of this size can be effectively treated in out-patient facilities. Larger lesions are better treated in an in-patient hospital setting, where medical CT [now almost always multidetector CT (MDCT)] and/or MRI are widely available. Asaumi and co-workers have revealed that the roles magnetic resonance imaging (MRI) can play in the differentiation between different lesions [4].

Although periapical radiolucencies of inflammatory origin (PRIOs) [6] are the most frequent lesions that present in

✉ David MacDonald
dmacdon@dentistry.ubc.ca

[1] Division of Oral and Maxillofacial Radiology, University of British Columbia, 2199 Wesbrook Mall, Vancouver, BC V6T 1Z3, Canada

[2] British Columbia Cancer Agency, Vancouver, Canada

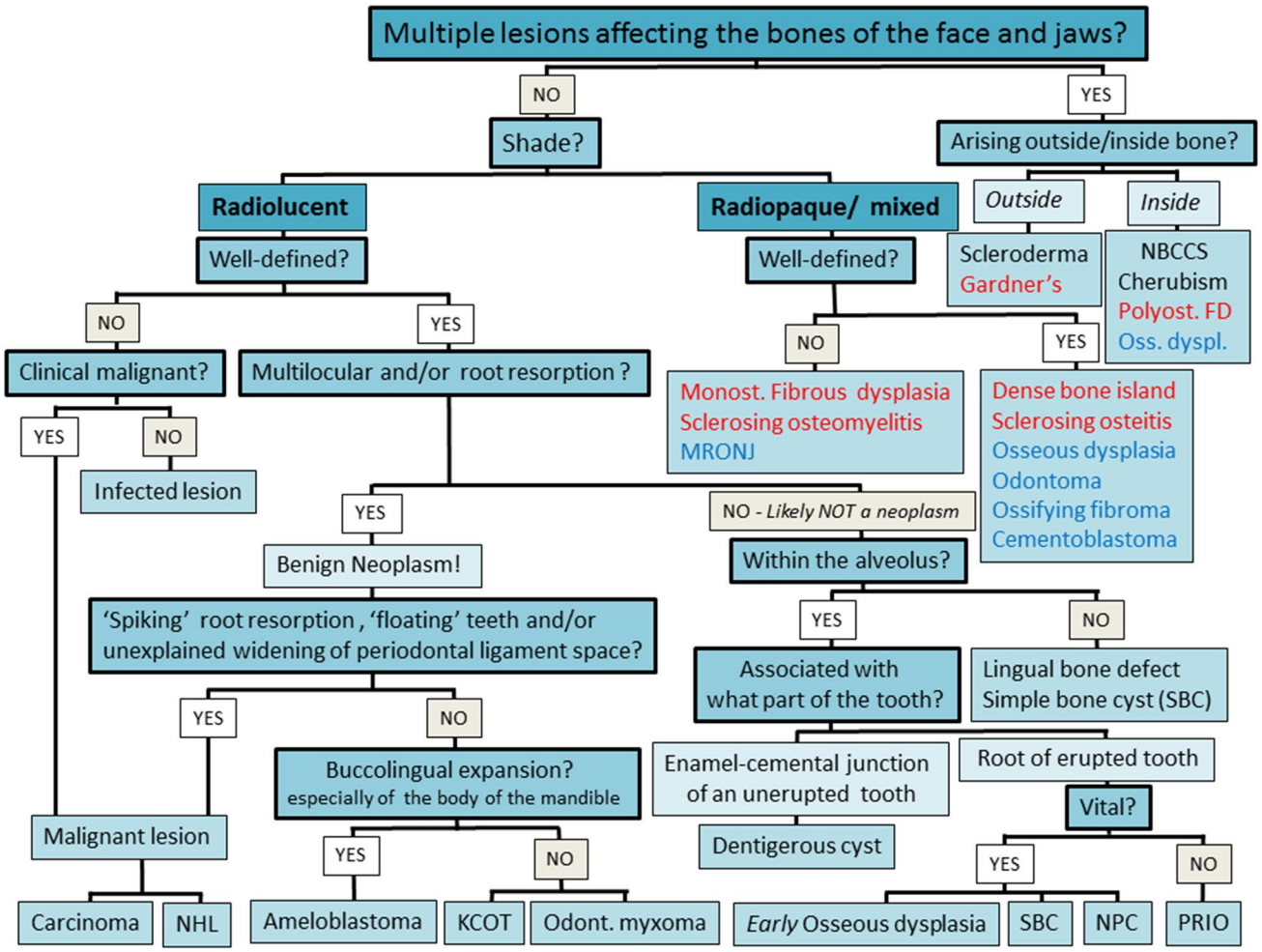

Fig. 1 Flowchart displaying the diagnosis of the most important and/or frequent lesions affecting the bones of the face and jaws, particularly when viewed initially on a panoramic radiograph. The contribution demographic, clinical features, and any subsequent cross-sectional imaging make to these diagnoses are discussed in the text. The most frequently found lesion that is most experienced in the practice of general dentistry is the PRIO (periapical radiolucency of inflammatory origin) has been deliberately left to last to encourage consideration of the other less common lesions, some which can have a potentially serious outcome on the patient particularly if not perceived and diagnosed promptly. All lesions which are radiolucent are in black text; those which are at all-times radiopaque are in red text and those which begin as radiolucencies and become radiopaque are in blue text. *KCOT* keratocystic odontogenic tumor (also called odontogenic keratocysts by some authorities.), *monost*. monostotic, *MRONJ* medicinal-related osteonecrosis of the jaws, *NBCCS* nevoid basal cell carcinoma syndrome (formerly called Gorlin–Goltz syndrome), *NHL* non-Hodgkin lymphoma, *NPC* nasopalatine duct cyst, *odont*. odontogenic, *Oss. dyspl* osseous dysplasia, *polyost. FD* polyostotic fibrous dysplasia, *PRIO* periapical radiolucency of inflammatory origin

dentistry there are many other lesions that should be considered first. The text will follow the flowchart in Fig. 1 by first addressing those lesions likely of systemic origin.

Multiple lesions within the jaw bones

Figure 1 begins at the very top with multiple discrete lesions. Such lesions are generally underpinned by a systemic disease process, and thus caution the primary care dentist, particularly those in general or family dentistry' that the treatment they deliver will be limited in scope and that the patient may need to be considered for referral to an appropriate specialist. Osteoporosis is generally osteolytic, and therefore, the jaws present radiologically more translucent. Although the OSTEODENT index predicts probability of a hip fracture caused by osteoporosis derived in part from a panoramic radiograph prospective trials are needed to confirm this finding and to determine its practicability in clinical dental practice [7].

Lesions may create changes in the jaws from outside or within the jaws. Scleroderma is an important example of

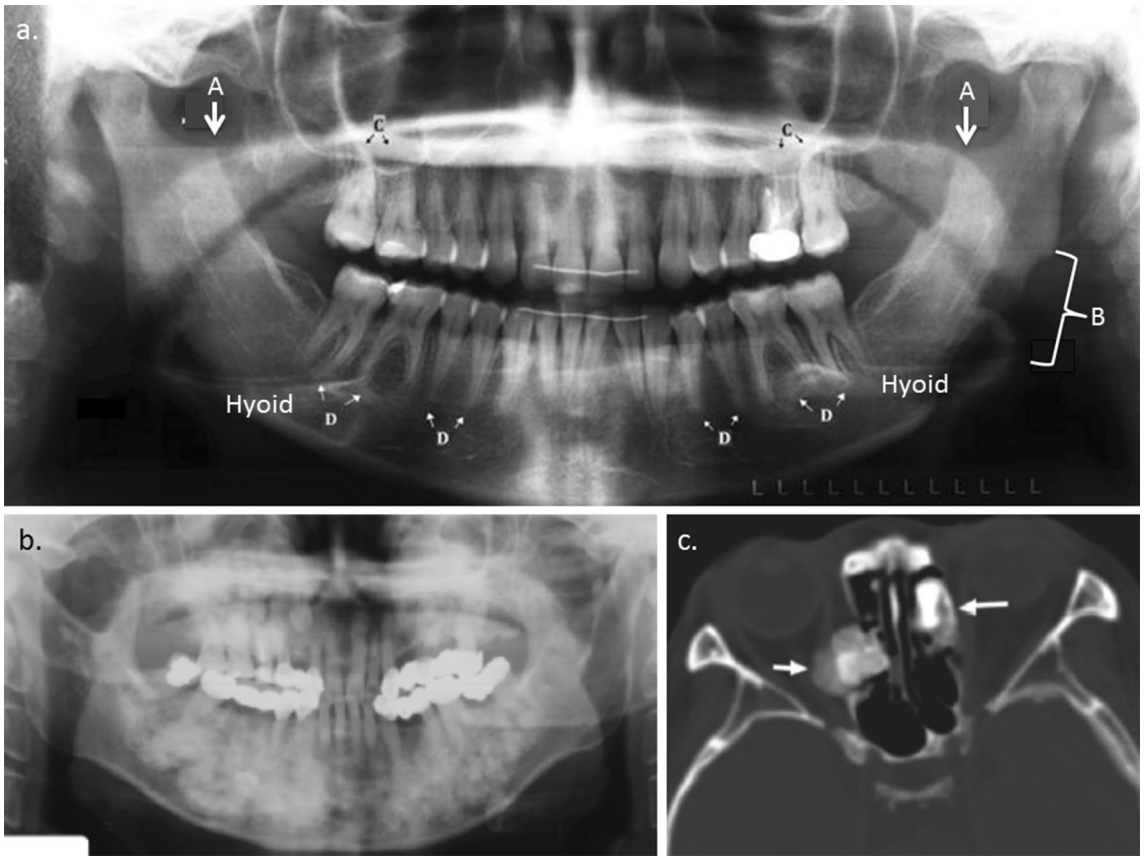

Fig. 2 **a** Panoramic radiograph of patient with scleroderma (systemic sclerosis) with severe erosions at (A) both coronoid processes and the adjacent anterior margins of the rami, (B) the left angle of the mandible. Also shown is the periodontal ligament space widening in (C) maxillary posterior teeth, and (D) mandibular posterior teeth. Note: the position of the hyoid bone is unduly high and may reflect the underlying scleroderma. **b, c** Panoramic radiograph and an axial computed tomograph of a patient diagnosed with Gardner's syndrome (polyposis coli). **b** Exhibits multiple osteomas in both the alveolar and basal processes of both jaws. The osteomas have almost completely obliterated the maxillary antrum. **c** Osteomas arising from the medial wall of both orbits (arrows). On the right, the lesion is displacing the medial rectus muscle laterally and slightly indenting the right optic nerve, producing mild proptosis. This lesion is separated from the adjacent bone by a radiolucent zone. Acknowledgements: **a** Dagenais et al. [2]. **b, c** Lee et al. [5]

the former resulting in the disappearance of the normal anatomical elements of the mandible, such the condylar and coronoid processes, angles, and parts of the ramus (Fig. 2a) [2]. Although most other changes are radiolucencies, the malignant transformation in the polyposis coli of Gardner's syndrome may be preceded by multiple osteomas in the jaws and other facial bones (Fig. 2b, c) [5].

Multiple radiolucencies particularly in the young may prompt consideration of cherubism (Fig. 3a) and multiple keratocystic odontogenic cysts (KCOT; also called 'odontogenic keratocysts'), suggestive of nevoid basal cell carcinoma syndrome (NBCCS; formerly called 'Gorlin–Goltz syndrome') (Fig. 3b–d) [8, 9]. This syndrome requires multi-disciplinary management, embracing many dental and medical specialties. Another cause is cherubism (Fig. 3a) [10]. Although the cherubism proband classically presents with bilateral and bimaxillary multilocular radiolucencies mainly in the posterior sextants, other family members of the proband upon investigation frequently present with atypical lesions, such as radiolucencies in the midline of the mandible [6]. The lesions in cherubism can cause ocular and respiratory problems, generally in the early stages. The latter is due to obstruction of the airway resulting from a backward displacement of the tongue or to an obstruction of the nasal passages. Lymphadenopathy may also occur in the early stages [10].

The degree of marginal definition or 'zone of transition' (as frequently called by medical radiologists) is the most important feature of a lesion presenting on CR. A lesion on a CR with a zone of transition 1 mm or less will appear well-defined, whereas as those greater will appear poorly defined (Fig. 4a) [11]. The latter presentation prompts consideration of a malignant or an infected lesion; the distinction is often provisionally made with regard to the lesion's

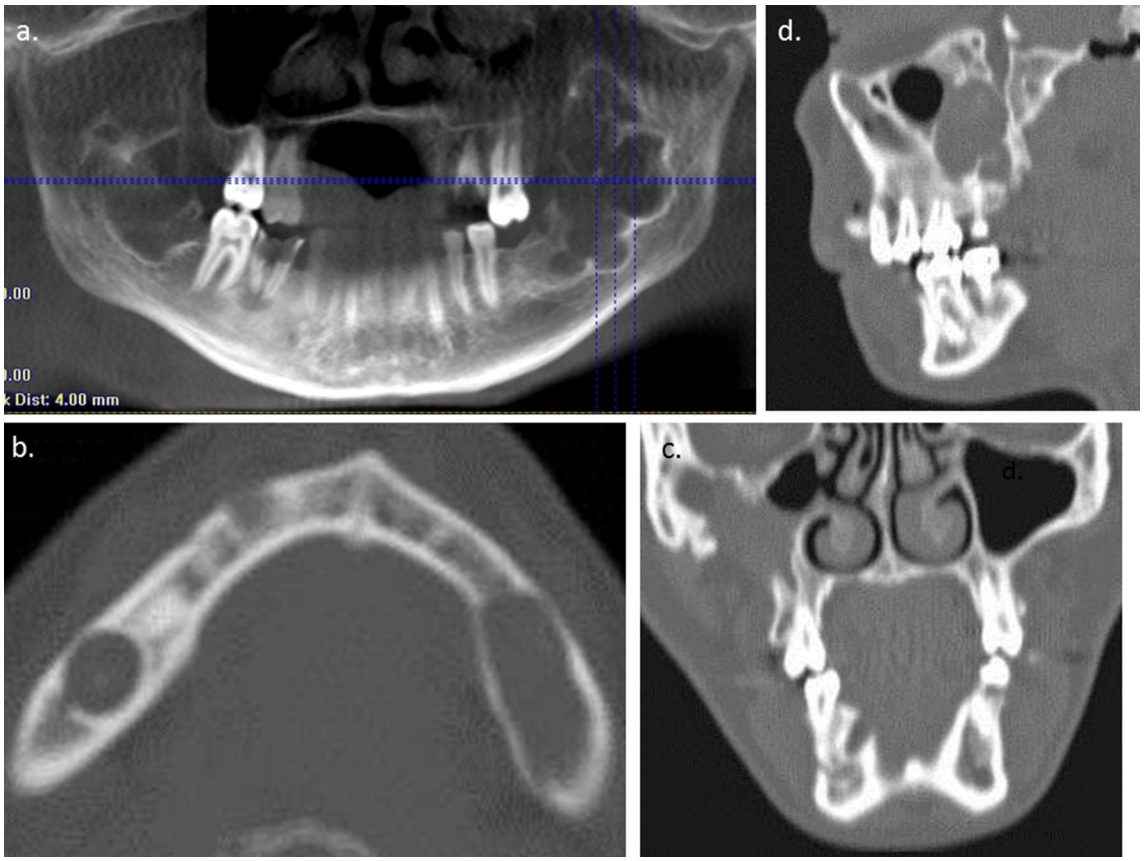

Fig. 3 Multiple lesions indicating a systemic cause. **a** Panoramic reconstruction from a cone-beam computed tomographic (CBCT) data set of a classical case of cherubism. This case displays a multilocular radiolucency in the posterior sextant of the mandible bilaterally. The left maxillary sinus has been substantially obturated by another lesion. The radiolucency at the lower right severely decayed first molar is a periapical radiolucency of inflammatory origin (PRIO). **b, c, d** are axial, coronal, and sagittal reconstructions respectively, of a CBCT data set of a case revealing multiple keratocystic odontogenic tumors (KCOT) associated with nevoid basal cell carcinoma syndrome (NBCCS). There are three in the mandible and one in the right maxillary sinus. The large KCOT on the left mandible displays minimal buccolingual expansion despite its extensive mesiodistal extent. The maxillary lesion displays a defect in the lateral wall caused by a biopsy. Therefore, some of the changes observed at that site may reflect the inflammation provoked by the biopsy rather than the original lesion. As far as possible biopsies and other surgery should be deferred until after all imaging has been completed. Some of the other major features of NBCCS are discussed in references [8] and [9] within the context of different in presentation between different ethnicities. Acknowledgement: MacDonald [6]

clinical presentation. A radiopaque lesion with a poorly defined margin on CR could be fibrous dysplasia (Fig. 4a) or sclerosing osteomyelitis (Fig. 6b). In those cases affecting the body of the mandible, the outline of the mandibular canal is enhanced by either lesion. This enhancement is due to the investment of the mandibular canal by dysplastic bone or osteosclerosis, respectively [11].

Polyostotic fibrous dysplasia manifests in the young patient (Fig. 4), with McCune–Albright syndrome presenting in the infant [12]. Fibrous dysplasia arising within the jaw bones presents on CR as a poorly defined lesion, observed on CR (Fig. 4a, b), whereas fibrous dysplasia arising elsewhere, namely, the appendicular skeleton, is usually well-defined. It should be noted that the poorer defined margins of fibrous dysplasia of the jaw on CR were not noted in MDCT reflecting the poorer spatial resolution of the latter (Fig. 4c–e) [13]. Nevertheless, the poorer defined margins may also be appreciated on CBCT when a higher spatial resolution is used; see both cases in Fig. 5. The difference between the gnathic and appendicular cases of fibrous dysplasia may reflect the fact that the bones of the jaws developed in membrane, whereas the most of appendicular skeleton developed by endochondral ossification. This supposition is supported by the presence of cartilage in fibrous dysplasia affecting the appendicular skeleton, but absent in those affecting the jaws [12].

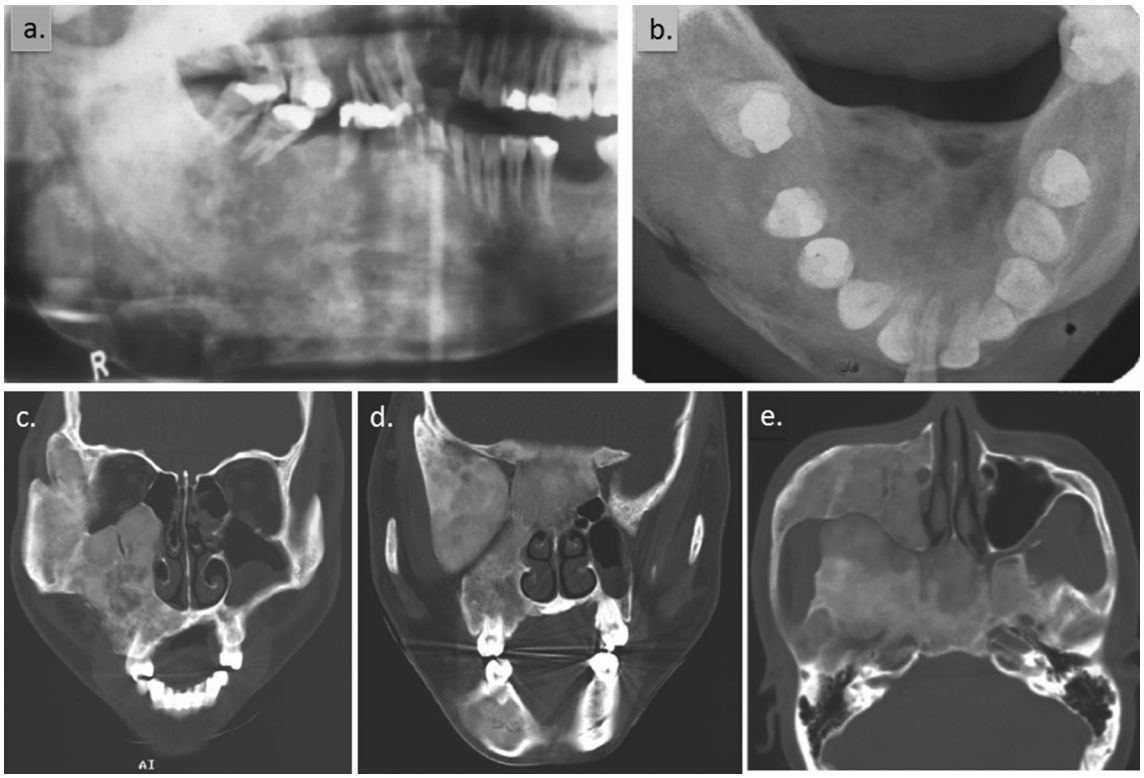

Fig. 4 Conventional radiography and computed tomography (CT) of a case of polyostotic fibrous dysplasia. **a** Conventional panoramic radiograph of a case of fibrous dysplasia affecting the right hemimandible and the right hemimaxilla. The right dysplastic lesion of the mandible has crossed the midline of the mandible. The midline has been denoted by the image of the post of the bite block. The boundary of the dysplastic bone is not readily distinguishable from the normal adjacent bone; the wide zone of transition between the dysplastic and normal adjacent bone means that there is poorly defined margin between them. The fusiform expansion of the mandible is obvious in the vertical dimension. The dysplastic lesions of both jaws have displaced the teeth towards each other resulting in an open bite of the largely unaffected left side. The lamina dura of the teeth within the affected regions are absent, in comparison with those in the unaffected regions. **b** True occlusal radiograph. The teeth still generally follow a catenary curve, although a central incisor has been displaced buccally. The patterns of the dysplastic bone vary throughout from ground glass, to 'peau d'orange' progressing from the right to left paramedial regions. The buccal dysplastic cortex is very thin in comparison with the normal contralateral side. **c** Coronal CT reconstruction at the level of the first premolar displaying fibrous dysplasia affecting both the right maxilla and zygomatic bone and extending upward to the frontal bone and medially into the hard palate. The right maxillary sinus is completely obliterated. **d** Coronal CT reconstruction posterior to that in c. now exhibiting a continuous fibrous dysplastic lesion affecting the maxillary, zygomatic, sphenoid, and ethmoid bones. The ethmoid air cells have been completely obturated. The superior and inferior orbital fissures, although narrower than the contralateral unaffected side, are, nevertheless, still patent. The affected right hemimandible exhibits substantial buccolingual expansion. **e** Axial CT reconstruction through the skull base. The maxillary sinus of the affected side has been completely obliterated by the fibrous dysplasia expanding outward both the anterior wall of the maxilla and the malar bone. Nevertheless, the inferior orbital canal has been preserved as has the diameter of the nasolacrimal duct. The latter has lost most of its cortex. The anterior portion of the lateral wall of the nasal cavity, although retaining its cortex has been displaced medially. Although the base of the skull has also been extensively affected, the ipsilateral zygomatic arch has not. Unlike the above canal and duct, the fibrous dysplasia has completely obliterated the foramen ovale and foramen spinosum. In addition, it has extended across the midline. The downwardly expanded base of the skull and the maxilla are still separated by the pterygomaxillary fossa now both narrowed and lengthened. Acknowledgement: MacDonald [11]

This leads onto the monostotic fibrous dysplasia affecting the face and jaws. This accounts for well over 90% of all such cases of fibrous dysplasia [12]. Figure 5 displays CBCTs of two such cases 5a and b affecting the mandible and 5c and d affecting the maxilla. Typically, only one side of the jaw is affected by fibrous dysplasia. Figure 5a, b displays a lack of lamina dura associated with tooth roots invested by dysplastic bone. Figure 5c, d exhibits the obturation of the maxillary sinus which was also noted in Fig. 4c–e. They are the two more important diagnostic features of fibrous dysplasia affecting the face and jaws. Figure 5c, d displays the sharply defined demarcation between a completely dysplastic bone, here the maxillary bone, and the adjacent normal bone, the zygomatic or malar bone precisely at the zygomatico-maxillary suture in a monostotic case, in comparison

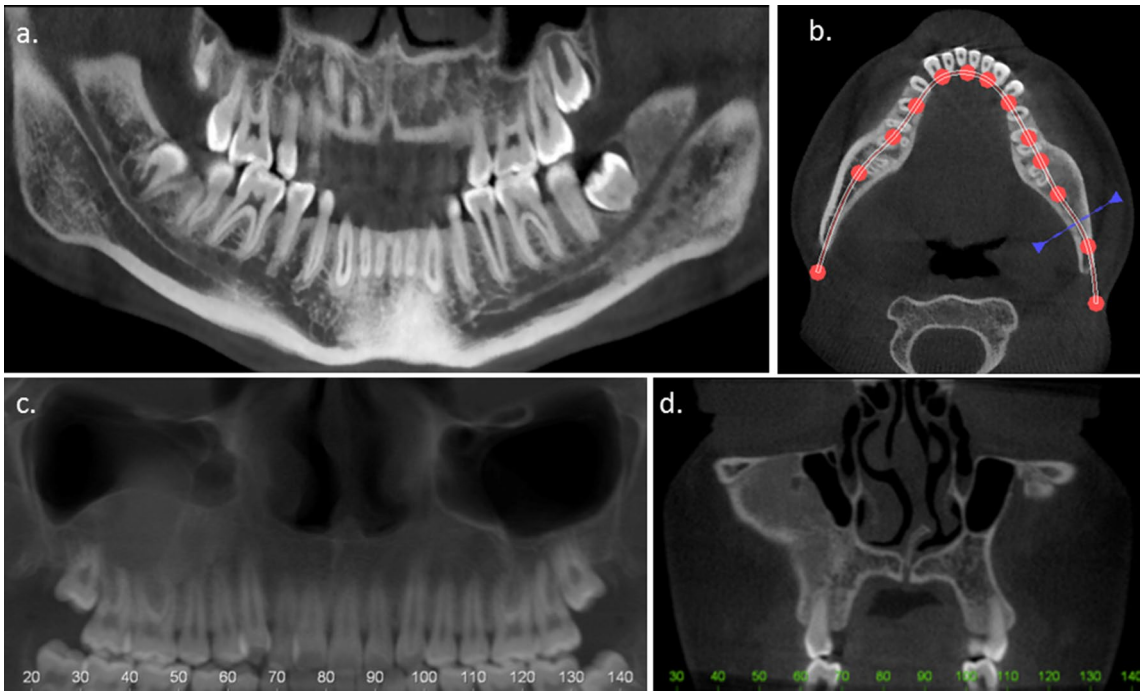

Fig. 5 Two cone-beam computed tomographic (CBCT) cases of monostotic fibrous dysplasia affecting the jaws; **a, b** of the posterior sextant of the left mandible and **c, d** of the right maxilla. **a, b** are panoramic and axial reconstructions, respectively, and **c, d** panoramic and coronal reconstructions, respectively. **a** Displays a replacement of the normal trabecular pattern seen on the right with a dysplastic pattern, mainly ground glass on the left. The cortices of the left mandibular canal have also been replaced by dysplastic bone making the translucent canal appear more apparent. **b** Reveals the slight fusiform buccolingual expansion. **c** Exhibits a fusiform dome-like upward expansion of the right maxillary alveolus. **d** at the level of the nasopalatine duct's origin at the floor of the nose, displays the expansion of the lateral wall of the maxillary sinus outward almost to the most lateral aspect of the malar (zygomatic) bone and inward into the sinus lumen, reducing the size of the air-filled sinus lumen. **d** also reveals that the dysplasia has not extending into the hard palate in this reconstruction, but has stopped at the zygomatico-maxillary suture. Acknowledgement: MacDonald [12]

with Fig. 4c–e, a polyostotic case in which these contiguous bones are both dysplastic.

Other diseases with multiple lesions affecting the jaws are florid osseous dysplasia and periapical osseous dysplasia. Since these are generally not accompanied by other lesions elsewhere in the body, they will be addressed in the next section addressing 'other radiopaque lesions'.

Other radiopaque lesions

Other radiopaque lesions that have poorly defined margins like fibrous dysplasia are sclerosing osteomyelitis (Fig. 6b) and medication-related osteonecrosis of the jaws (MRONJ) (Fig. 7). Although both sclerosing osteomyelitis and MRONJ can display a zone of sclerosis (increased radiopacity) extending outside the alveolus into adjacent basal bone, some buccolingual expansion (due to new bone formation) and a sequestrum (an island of dead bone), all three are generally viewed together in MRONJ. The MRONJ can arise when antiresorptive agents, such as bisphosphonates and denosumab, were used to treat osteoporosis or oncology patients [14]. A long term Japanese study reported that although bisphosphonates delay tooth-socket healing, they did not cause a single case of MRONJ [15]. CBCT was used to predict future bone exposure of Stage 0 MRONJ by identifying radiographic sequestration [16].

The rest of the radiopacities are well-defined. The majority is either areas of sclerosing osteitis, which occur secondary to pupal necrosis (Fig. 6b), or dense bone islands. Although the dense bone island is considered idiopathic (that is having no known cause), hence, its alternative name of idiopathic sclerosis, a relation between its size and its prevalence and the concentration of fluoride in the water were discussed in one report [20]. This report included an East Asian community [20]. Both sclerosing osteitis and dense bone islands can be further distinguished from the other well-defined radiopacities as their trabeculae are continuous with the adjacent normal bone, whereas the rest are generally separated from the adjacent bone by a capsule

Fig. 6 Conventional radiography of three cases displaying some of the more classic causes of radiopacity in the jaws. **a** (Periapical radiograph) and **b** (panoramic radiograph) display a cementoblastoma, sclerosing osteitis secondary to dental caries and localised sclerosing osteomyelitis; **c** (panoramic radiograph) and **d** (true occlusal radiograph) another cementoblastoma and **e** (periapical radiograph) a compound odontoma. **a** displays the cementoblastoma in **b** year earlier. It has already resorbed the mesial root and is fused to it. **b** Cementoblastoma in **b** is now resorbing and fusing to the apex of the distal root. The apical radiopacity on the carious first premolar is sclerosing osteitis in response to a necrotic pulp. The radiopacity within the bone extending from the second molar forward and down below the mandibular canal is a sclerosing osteomyelitis. **c, d** is another case of a cementoblastoma which has expanded centrifugally in all dimensions and has extended downward past the mandibular canal into the basal process of the mandible. This large cementoblastoma is also associated with a sclerosing osteomyelitis. The mandibular canal associated with both cementoblastomas is as a result more obvious and translucent than it would appear if it were invested in normal bone. **e** Is of a compound odontoma in the anterior maxilla hampering the eruption of the erupting permanent canine. This lesion classically presents as a 'bag of teeth' (denticles) as it does here. Acknowledgements: **a–d** MacDonald-Jankowski and Wu [17]. **e** MacDonald-Jankowski [18, 19]

[11]. These encapsulated lesions are osseous dysplasias (Figs. 8, 9, 10), cementoblastomas (Fig. 6a–d), odontomas (Fig. 6e), and ossifying fibromas (OF) (Fig. 11). The only exception to this is the juvenile variants of OF (Fig. 11d, e), which do not generally display capsules. This absence of a capsule may account for their higher recurrence, due to the difficulty, during surgery, of the surgeons detecting a clear boundary between the normal adjacent tissues and the lesion [12].

Osseous dysplasia is prevalent in middle-to-old-aged females of East Asian and Sub-Saharan African origin presenting as one of two variants; the florid variant (affects more than one sextant; Figs. 8, 9) or the focal variant (a single or multiple adjacent lesions confined to a single sextant; Fig. 10) [12]. Osseous dysplastic lesions begin as radiolucencies which undergo central mineralisation (Fig. 8) [12]. Although these generally require no treatment, they pose problems if they become secondarily infected. Furthermore, their presence in the edentulous alveolus contraindicates implant placement [11]. Therefore, avoidance of these difficulties may be achieved by retention of the associated teeth. Therefore, non-vital teeth or those of questionable vitality should be referred to endodontists for treatment. In very rare cases, these lesions may expand massively necessitating

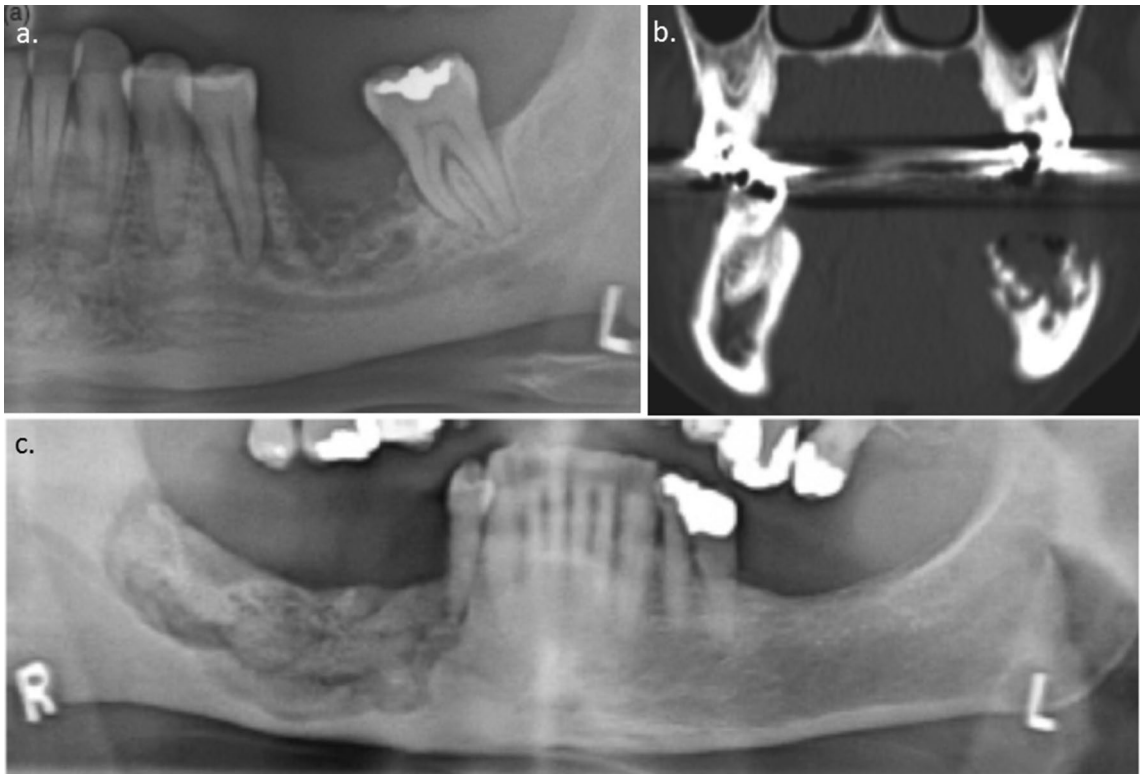

Fig. 7 Two cases of medication-related osteonecrosis of the jaw (MRONJ). **a** Panoramic radiograph of MRONJ in the lower left molar area. Although the most obvious element of the two cases are the sequestra, these do not encompass the entire lesions which include the increased and diffuse radiodensities extending into the basal processes of the each mandible. Sequestra are observed above the mandibular canal (MC). The MC is made more apparent by the increased radiopacity of the bone investing it. **b** Coronal section of a computed tomograph through the same site in **a**. The sequestra are again observed along with the increased density of the medulla of the mandible and an expansion of the mandible in comparison with the normal unaffected contralateral side. **c** Panoramic radiograph of MRONJ in the lower right mandible. The MRONJ is more extensive mesiodistally and vertically, extending well down into the basal process of the mandible. Again, the MC is more visible in the affected side than in the unaffected side. Acknowledgement: MacDonald [11]

ablative surgery. Reports of expanding osseous dysplasia (EOD: also called by some gigantiform cementoma) [21] are now found in all ethnicities and affect both genders. There is yet another variant, which though reported in all ethnicities, is most prevalent in young females of European origin. It is non-expanding. It is periapical osseous dysplasia (POD; formerly called periapical cemental dysplasia) [12]. POD presents initially as multiple juxtaposed periapical radiolucencies confined to the lower anterior sextant (Fig. 10). Its early radiolucent stage may occasionally prompt unnecessary endodontic treatment. Well-defined radiopacities that exhibit buccolingual expansion, root resorption and/or tooth displacement are OF (Fig. 11).

Malignant lesions

The most important feature particularly in radiolucent lesions is marginal definition or zone of transition defined earlier. A lesion presenting on CR with a zone of transition greater than 1 mm is generally considered to be either a malignant (Fig. 12) and/or an infected lesion (Fig. 13a). Although the former are the most important, the clinical examination and history generally determine the provisional diagnosis. Nevertheless, even if the lesion appears well-defined, if it displays 'spiking' or 'spiked' root resorption (Fig. 12c), 'floating' teeth (Fig. 12a, c) or an unexplained widening of the periodontal ligament space, then a malignant lesion should be considered. The most frequent malignancies of the face and jaws are carcinomas or non-Hodgkin lymphomas (NHL) (Fig. 12). Although both principally arise intraorally within the mucosa, the latter predominantly from the lymphoid tissue in the tonsil (lingual, palatine or pharyngeal), a minority arise within the alveolus; the carcinomas from epithelial remnants of odontogenesis (primary intraosseous squamous cell carcinoma) [11] and the NHLs from lymphocytes within the alveolus associated with dental infections in some cases [22, 23]. Kato et al. reported the advanced imaging differences between SCC and NHLs arising within the sinus [24].

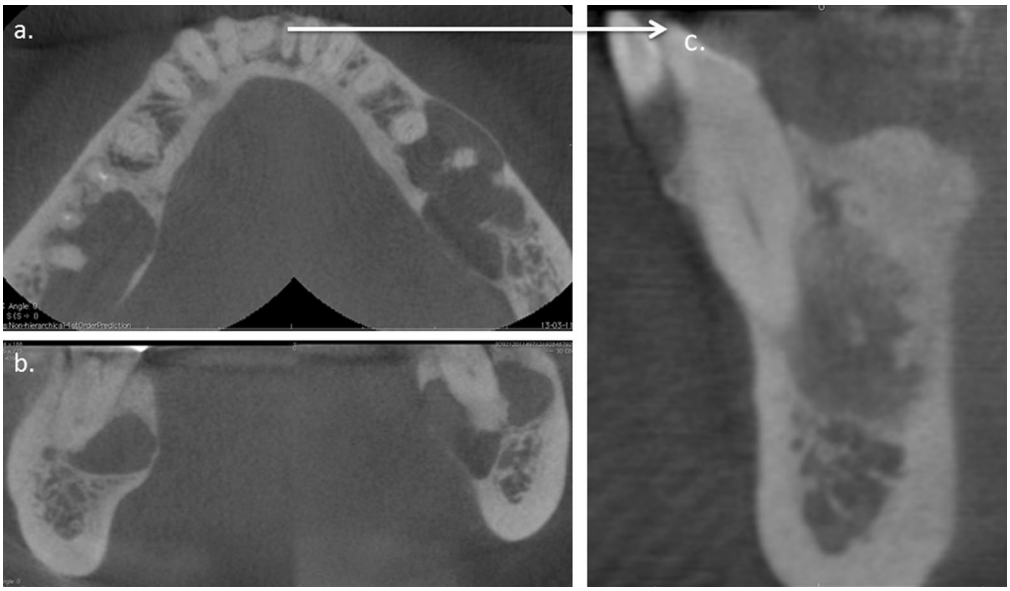

Fig. 8 Cone-beam computed tomographic (CBCT) case of florid osseous dysplasia of an East Asian middle-aged female exhibiting lesions affecting all three sextants of the mandible. **a**–**c** Axial, coronal, and transaxial reconstructions, respectively. **a, b** Well-defined radiolucency in the posterior sextant bilaterally. Although both lesions exhibit minimal buccolingual expansion they reveal erosions of the contiguous cortices. Each lesion envelopes a tooth root, whose apex is invested in a calcified mass separated from it by a thin radiolucent line in line with the periodontal ligament spaces. The right central incisor in a. is displayed in **c** as having a well-defined substantially ground glass apically. Within this lesion, there are a few more radiodense flecks. Again the continuous cortices are eroded, but not displaced. Acknowledgement: MacDonald [12]

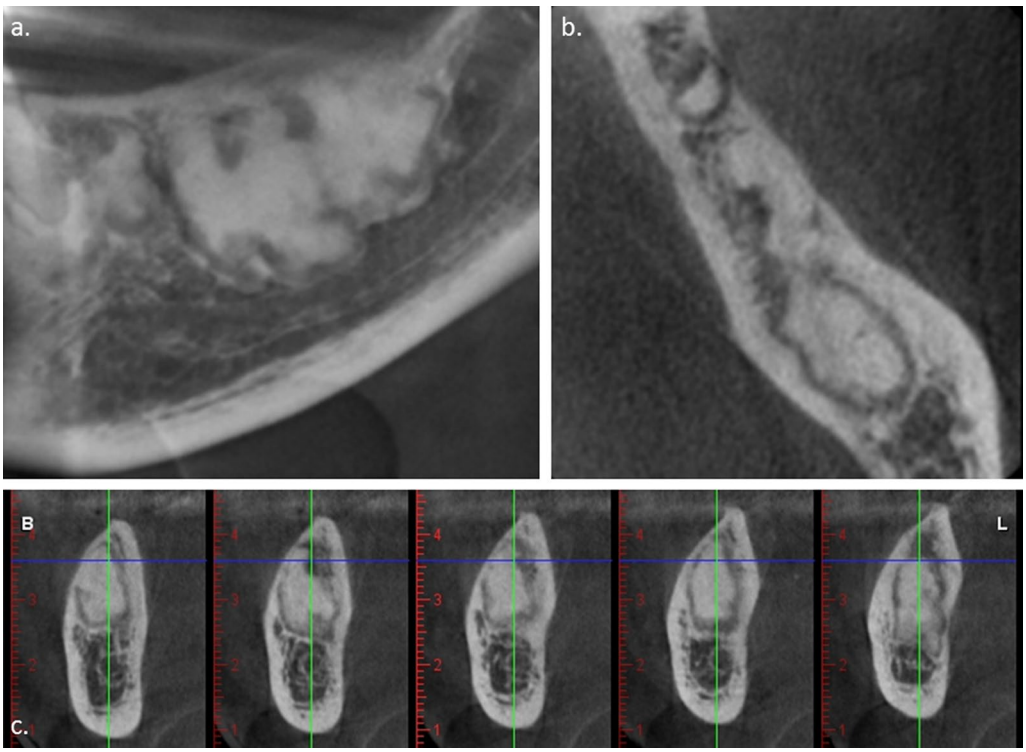

Fig. 9 Small field-of-view cone-beam computed tomographic (CBCT) case of florid osseous dysplasia of the left mandibular sextant in a middle-aged East Asian female. The conventional panoramic radiograph had displayed lesions in all posterior sextants. **a**–**c** Panoramic, axial, and transaxial reconstructions, respectively. The reconstruction program was 'curved' akin to computed tomography 'dentoscan'. They all reveal radiopacities within the edentulous alveolus. There is no buccolingual expansion. Acknowledgement: MacDonald [12]

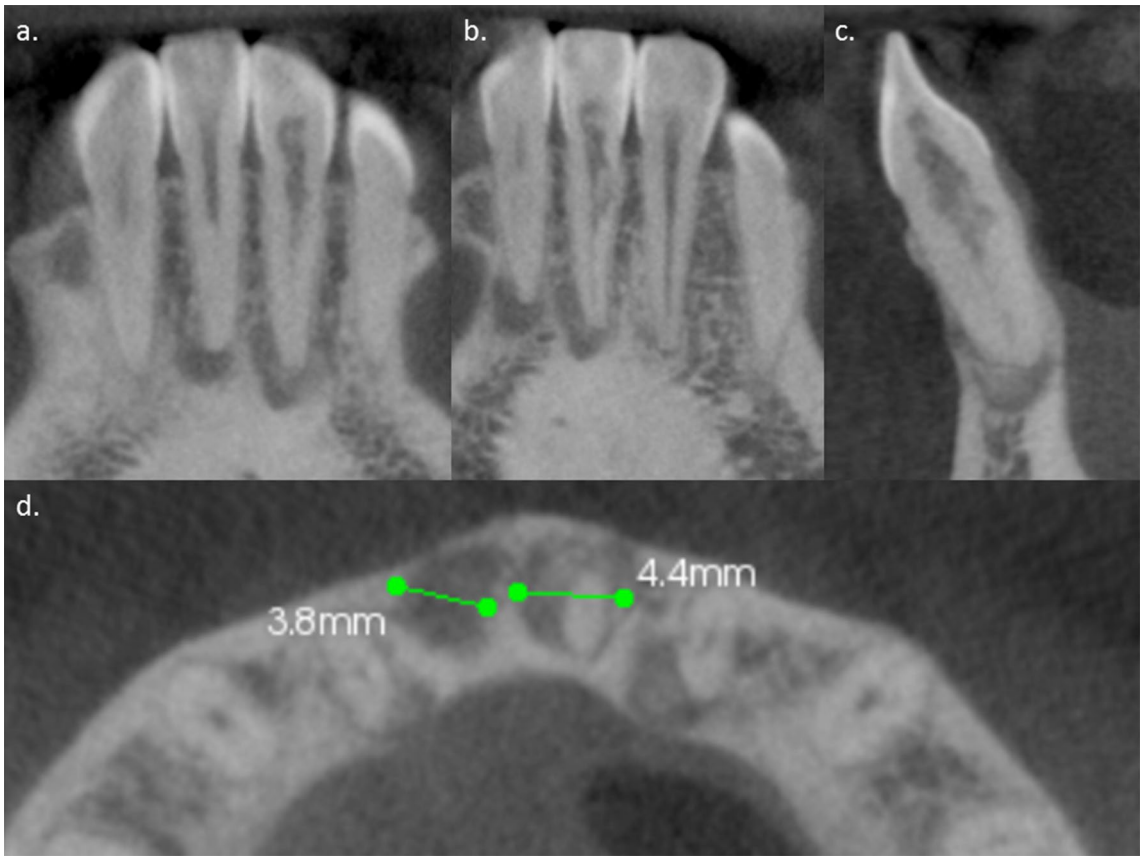

Fig. 10 Small field-of-view cone-beam computed tomographic case (CBCT) of periapical osseous dysplasia of the anterior mandibular sextant in a young adult female of European origin. **a**–**d** Coronal, sagittal, and axial reconstructions, respectively. The reconstruction program was 'multiplanar reconstruction or reformatting (MPR),' the standard reconstruction for computed tomography. **a**–**c** Periapical radiolucencies with central opacities. They also reveal internal resorption of the dental pulp canals. **d** Reveals that the diameters of the lesions are less than 0.5 cm and cause no buccolingual expansion. Acknowledgement: MacDonald [12]

Benign neoplasms

The next stage is the determination as to whether the lesion is a benign neoplasm or a cyst, because the former may recur, particularly after conservative treatment (e.g., enucleation), which is more effective for treating cystic lesions. Although a multilocular appearance (Fig. 14a, b) and/or the presence of root resorption (Fig. 14c) determine the former, their absence does not rule out consideration of a neoplasm [6]. Lesions that arise or are observed to be substantially confined to the alveolus (in the mandible above the mandibular canal, which separates the tooth-bearing alveolus and the basal process) are most likely to be odontogenic. These are either odontogenic neoplasms, such as the ameloblastoma (Fig. 14), KCOT (Fig. 15) and odontogenic myxoma (Fig. 16), or odontogenic cysts such as dentigerous cyst (Fig. 17), radicular cyst (Fig. 18a, b). Other causes are nasopalatine duct cyst (Fig. 18c, d) and/ or early stage dysplastic lesions such as osseous dysplasia (Fig. 8a) [6]. In addition to some subtypes of neoplasm such as the unicystic ameloblastoma (Fig. 14e), which have a substantial cystic component, other odontogenic neoplasms in their early stages may appear unilocular and if they secondarily envelop the crown of an unerupted tooth they need to be distinguished from the dentigerous cyst. The dentigerous cyst is attached to the enamel–cemental junction (Fig. 17a) or within a millimeter apical to it (Fig. 17c), any other relationship should be considered neoplastic. KCOTs, arising the posterior maxilla, are often observed expanding upward into the sinus lumen carrying with them an unerupted third molar. Figure 15c, d displays a KCOT, though arising in the anterior maxilla, has extended sufficiently posteriorly to exhibit a balloon-like expansion of the sinus' anterior wall and adjacent floor (Fig. 15c) [6].

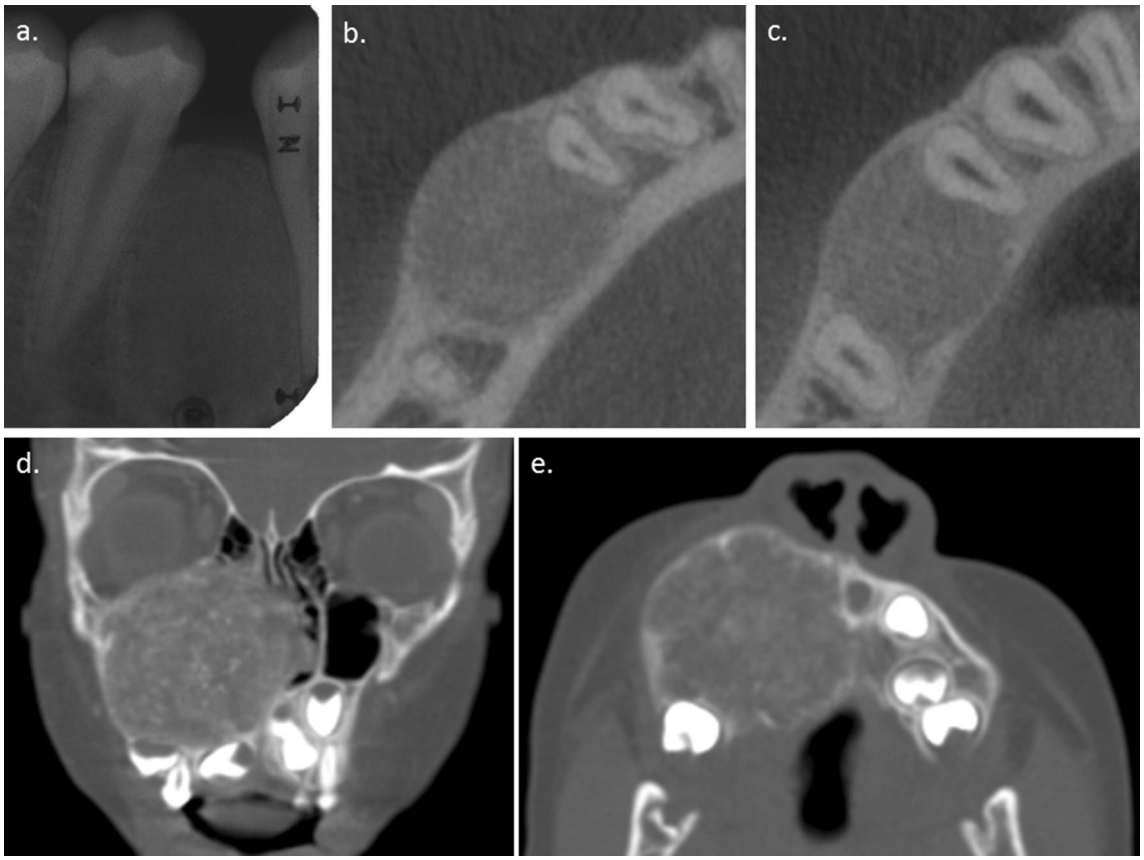

Fig. 11 Two cases of ossifying fibroma. **a** Periapical radiograph displaying a thin capsule as a black line running around the periphery of the ossifying fibroma. This is even also seen in the distal aspect of the lesion in **b**. **b, c** Axial reconstructions of cone-beam computed tomography also reveal buccolingual expansion in addition to the tooth displacement obvious in **a**. **d, e** are coronal and axial sections respectively of computed tomography of a case of juvenile ossifying fibroma. This large spherical lesion almost completely occupies the right maxilla. Although well-defined it is not encapsulated unlike the conventional ossifying fibroma in **a**–**c**. Acknowledgement: MacDonald [12]

Expansion of a lesion is indicative of its nature. Almost all neoplasms and all true cysts exhibit expansion due to their centrifugal growth occasioned by cell division in the former and hydrostatic pressure in the latter. Nevertheless, there are different expansive shapes. Most neoplasms, including the ameloblastoma, and cysts exhibit a 'beach-ball-like' expansion (Figs. 14a, e, 17c, d, 18), whereas KCOT and odontogenic myxomas, particularly those affecting the body of the mandible (Figs. 15a, b, 16a–c), are more fusiform, as they extend more mesiodistally through the medullary cavity rather than expand buccolingually. This is due, in part, to the KCOT's low soluble protein content and, therefore, low hydrostatic pressure in conjunction with the thick cortices of the mandible, whereas in the case of the myxoma, this is due to both the lack of a capsule and its gelatinous consistency. In the maxilla, where the cortices are thinner and are adjacent to air-filled spaces, these lesions' expansive growth is less inhibited (Figs. 15c, d, 16d) [6].

CBCT has come to the dentist's assistance for the diagnosis and assessment of some lesions without a need for a surgical investigation. Two such lesions that may be effectively diagnosed in this way are the lingual bone defect and some simple bone cysts (Fig. 19). The former is unique to the jaws, whereas the latter is also found elsewhere in the skeleton and is known by many names, such as traumatic bone cyst and solitary bone cyst. The lingual bone defect excavates the medullary cavity of the basal process of the mandible and in some cases erodes and displaces the buccal cortex when reached. Not only does lingual bone defect occur in middle age, so far, there has only been one published report of it

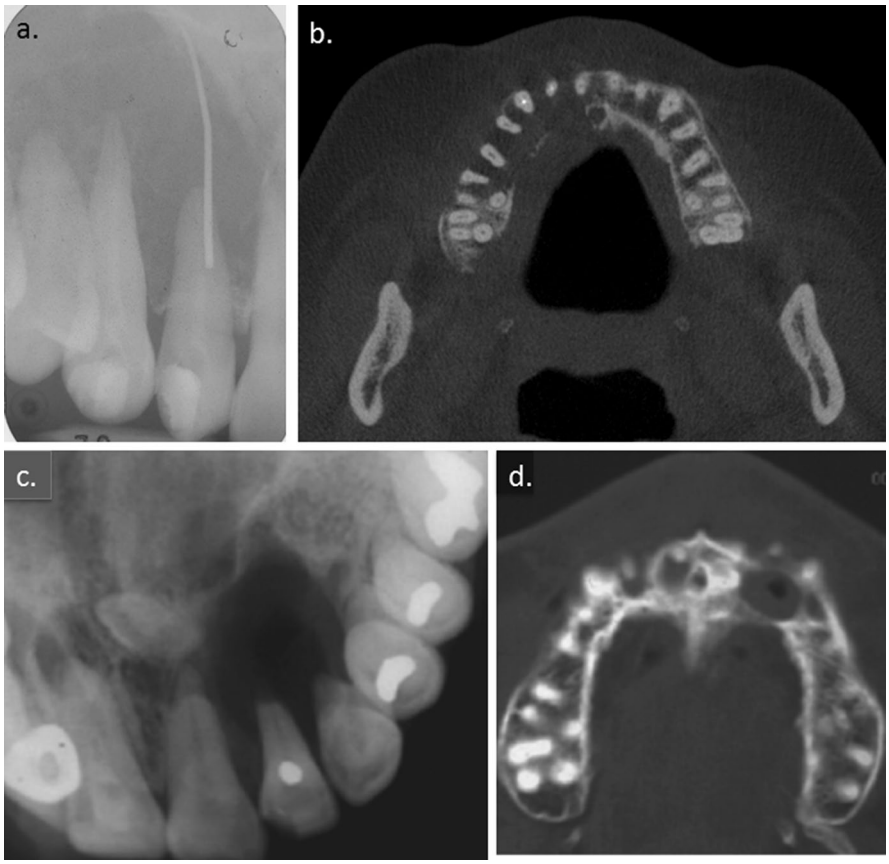

Fig. 12 Two cases of malignant lesions arising in the maxillary alveolus; a non-Hodgkin lymphoma (NHL; **a, b**) and a carcinoma (**c, d**). **a** Periapical of an NHL which has substantially removed the bone around the roots of the right anterior and first premolar teeth. **b** Axial reconstruction of the cone-beam computed tomographic (CBCT) data set. The lesion extends from the nasopalatine foramen back to the right second molar tooth removing both the trabeculae and cortices. **c** Standard anterior occlusal of a carcinoma exhibiting a well-defined, but irregular radiolucency associated with floating teeth with a 'spiked' resorption of the roots particularly of the left canine and lateral incisor. **d** Computed tomographic axial reconstruction of the lesion in **c**. Acknowledgement: MacDonald [22]. **c, d** MacDonald [11]

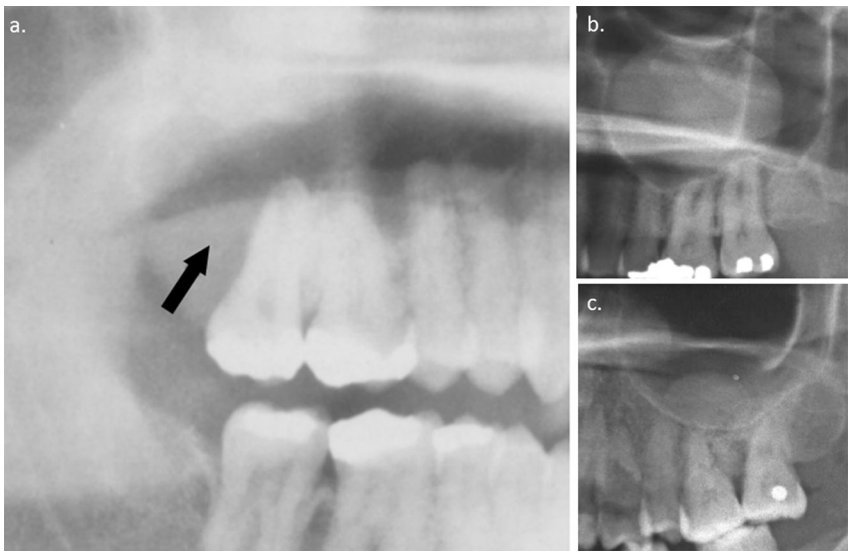

Fig. 13 **a** Panoramic radiograph displaying an infected keratocystic odontogenic tumor affecting the maxillary sinus (MS). The MS displays a soft-tissue radiopacity. There is no cortex at the maxillary tuberosity and adjacent posterior antral wall (arrow). This provoked consideration of a squamous cell carcinoma as the provisional diagnosis. **b** Panoramic radiograph exhibiting a mucosal antral pseudocyst substantially obturating the maxillary sinus. The subjacent teeth are both caries-free and display only small restorations. Nevertheless, the vitality of these subjacent teeth should be confirmed prior to a diagnosis of a mucosal antral pseudocyst. Non-vital teeth would suggest that the lesion would be rather a mucosal reaction to a periapical infection. **c** Panoramic radiograph of multiple dome-shaped structures. The one arising from the floor of the sinus alone is presenting alone would be indistinguishable from the lesion in b., but multiple such lesions is suggestive of chronic sinusitis. A history of the last is often present. Acknowledgement: MacDonald [11]

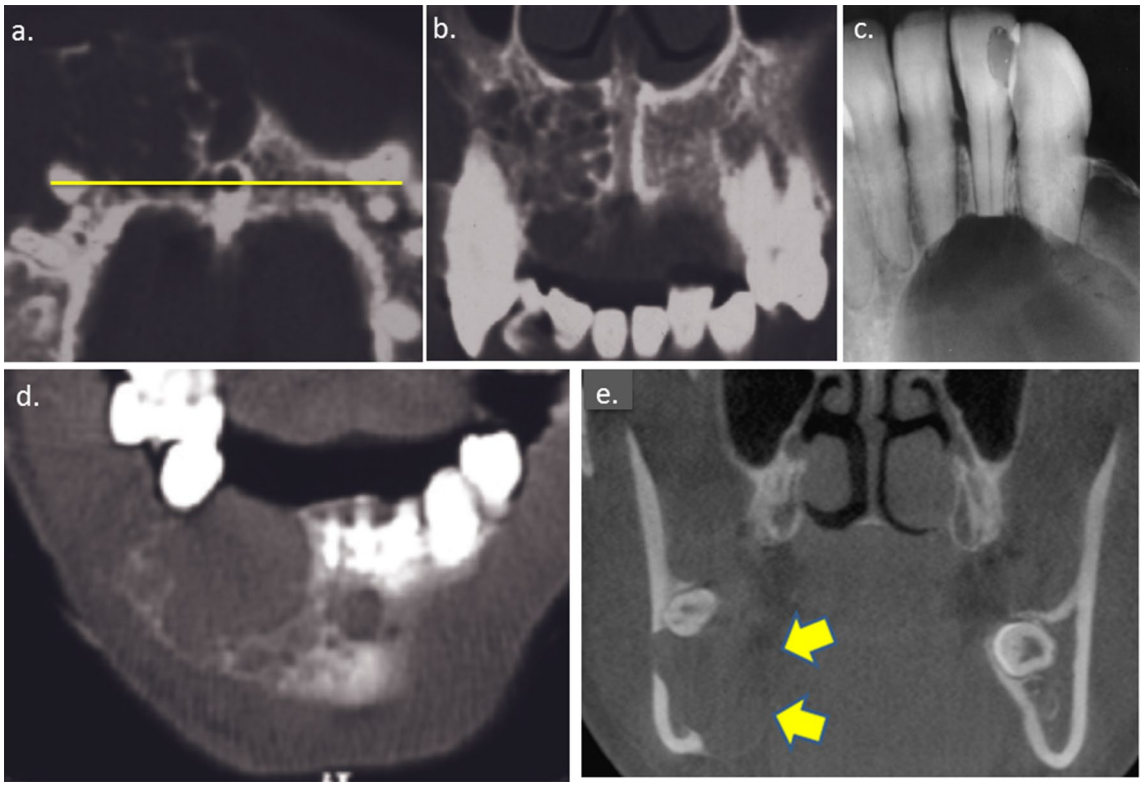

Fig. 14 Four cases of ameloblastoma; three solid ameloblastoma (**a**–**d**) and a unicystic ameloblastoma (**e**). **a** Bone window of an axial computed tomograph (CT) of a solid ameloblastoma in the anterior maxilla. It is multilocular (mainly soap-bubble) and exhibits buccolingual expansion. **b** Coronal section of the same case at the level of the yellow line in **a** through the nasopalatine duct displaying a honeycomb multilocular pattern. It reveals erosions of the nasopalatine duct, floor of the nose and floor of the anterior aspect of the maxillary sinus. **c** Periapical radiograph of an ameloblastoma affecting the premolar–molar area of the mandible. It displays marked resorption of the roots of the affected teeth. **d** Coronal CT section of an ameloblastoma in the anterior mandible revealing both soap-bubble and honey-comb multilocular patterns; the latter is towards the midline. **e** Coronal reconstruction of the cone-beam CT of a unicystic ameloblastoma in the posterior mandible. It displays substantial erosion and expansion, particularly of the lingual cortex (arrows). Acknowledgements: **a, b, d** MacDonald [11]. **c** MacDonald-Jankowski et al. [25]. **e** MacDonald [6]

causing a pathological fracture in a Japanese patient [28]. This lack of a propensity to fracture is surprising due to the considerable excavation of the body of the mandible, such as that in Fig. 19d–f. This lack of fracturing may reflect older age of onset. This older age may be associated with less of the risk-taking observed in the young. Some lingual bone defects, rather than presenting adjacent to the submandibular gland, present adjacent to the sublingual gland and, therefore, involve the premolar alveolus and need to be distinguished from other lesions; the CBCT again proves invaluable for this task.

Although the mucosal antral pseudocyst (Fig. 13b) and sinus polyps (Fig. 13c), arising within the mucosa of the maxillary sinus, outside the maxillary alveolus, are

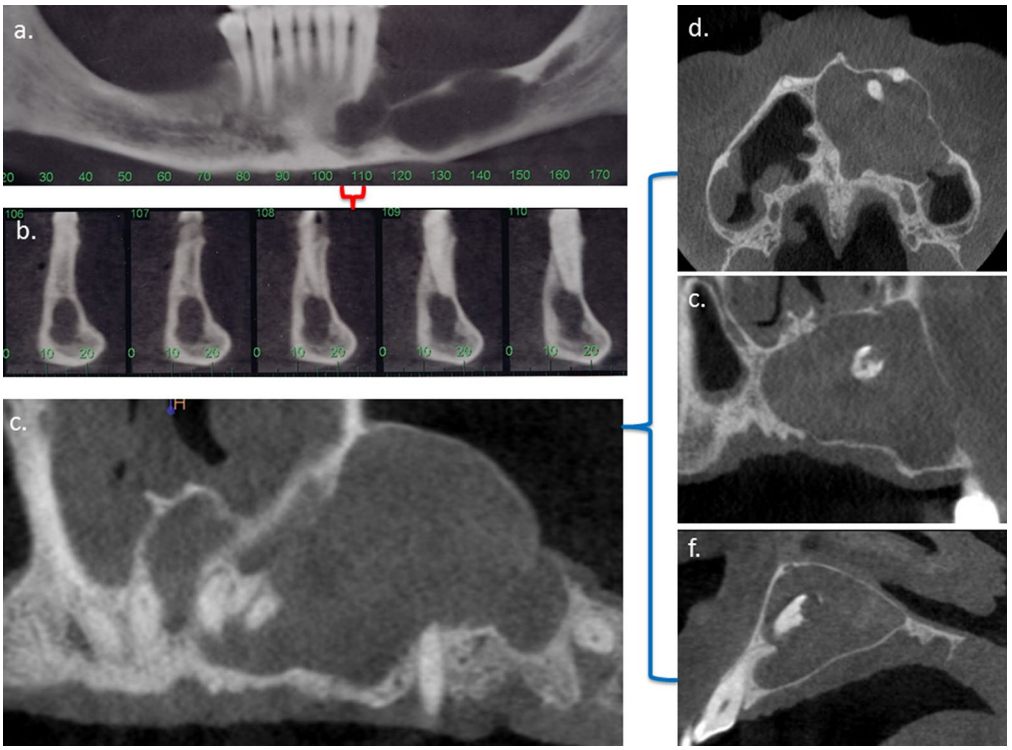

Fig. 15 Two cone-beam computed tomographic (CBCT) cases of keratocystic odontogenic tumors (KCOT; also known as odontogenic keratocysts by some authorities); **a, b** of a case affecting the mandible and **c**–**f** affecting the anterior maxilla. **a** Panoramic reconstruction and **b** is the transaxial reconstruction derived from the region indicated in **a**. Although the KCOT is mesiodistally very extensive, it is minimally expansive buccolingually. **c** Panoramic reconstruction of a KCOT in the anterior maxilla. **d**–**f** Reveal the presence the crown of an unerupted tooth within the lesion. **d** Exhibits some buccolingual expansion; it is not ball-like when reviewed in conjunction with **f**. The slightly greater expansion for the case in **c**–**f** than that for **a** and **b** reflects the thickness of the cortex in the body of the mandible in contrast to that in the anterior maxilla. Nevertheless, the distally most part of the KCOT (in **c**) is expanding balloon-like into the maxillary sinus reflecting the minimal resistance the floor of the sinus and air-filled sinus lumen presents to a growing KCOT. Acknowledgement: MacDonald [6]

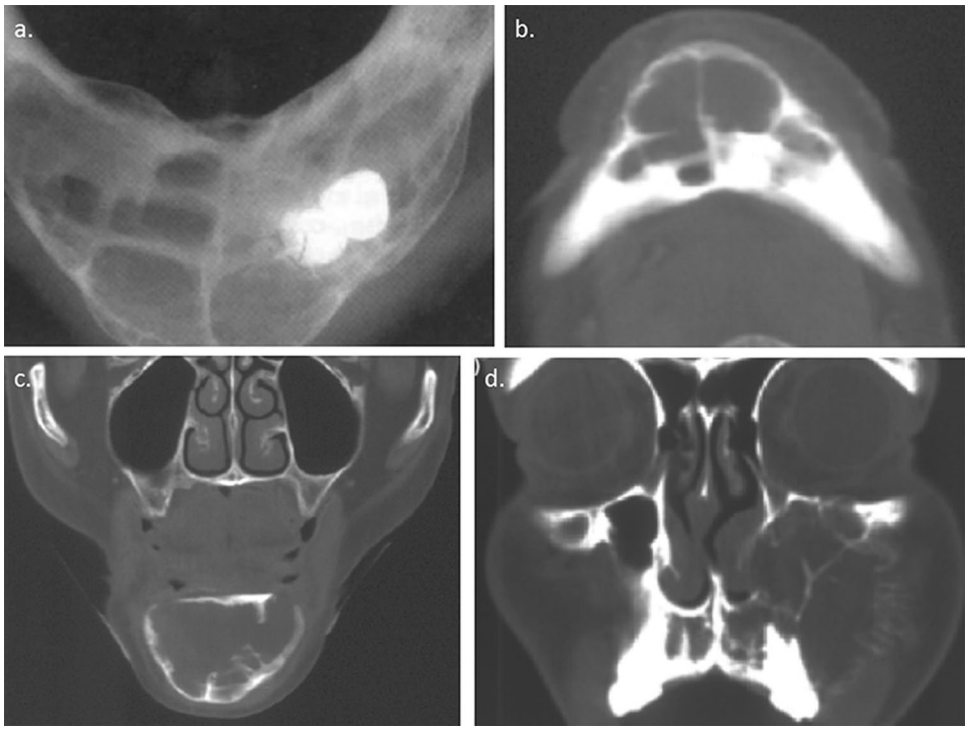

Fig. 16 Two cases of an odontogenic myxoma; a mandibular case (**a**–**c**) and a maxillary case (**d**). **a** True occlusal radiograph of a lesion in the anterior mandible exhibiting the classical 'tennis-racket' appearance pathognomonic for this lesion. This pattern is also appreciated in the axial and coronal computed tomographic sections of the same patient. The lesion effects a more fusiform expansion rather than the ball-like expansion of the ameloblastoma (Fig. 14) reflecting its lack of a capsule and its lava-flow like extension throughout the medullary cavity of the mandible. **d** Reveals a large soap-bubble like appearance medially in the maxillary lesion and a sun-ray like appearance more laterally. Acknowledgements: **a** MacDonald-Jankowski et al. [26]. **b**–**d** MacDonald-Jankowski et al. [27]

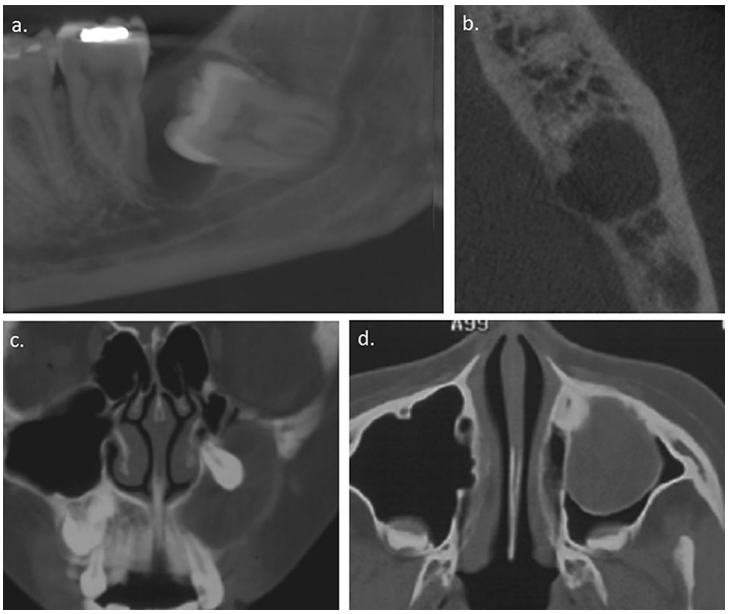

Fig. 17 Two cases of dentigerous cysts; the mandibular third molar (**a, b**) and a maxillary premolar (**c, d**). **a, b** Panoramic and axial reconstructions of a cone-beam computed tomographs (CBCT) data set. They display a well-defined coronal radiolucency attached the enamel–cemental junctions. **a** Displays that the adjacent second molar tooth is devoid of a lamina dura, whereas **b** reveals that the lingual cortex has been substantially eroded. **c, d** are bone-window coronal and axial computed tomographic sections, respectively. **c** reveals the cyst arising from the enamel–cemental junction (below the crown in **c**) or from the root within a millimeter from it (above the crown in **c**). The cyst has substantially obturated the lumen of the maxillary sinus and displaced and eroded its lateral wall. The roots are within the medial wall. **d** exhibits the cyst is unilocular and corticated. There is a residual air-filled space posteromedially and adjacent to the posterolateral wall which remains undisplaced. Acknowledgements: **a, b** MacDonald [6]. **c, d** [11]

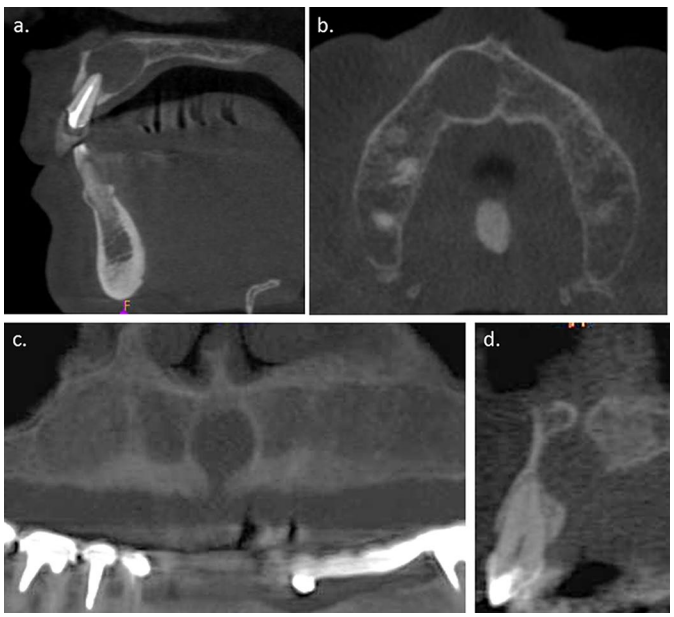

Fig. 18 Cone-beam computed tomographs (CBCT) of two lesions; a periapical radiolucency of inflammatory origin (PRIO; **a, b**) and a nasopalatine duct cyst (**c, d**). **a, b** are sagittal and axial reconstructions, respectively. They exhibit a well-defined unilocular corticated radiolucency associated with the apex of an already endodontically treated maxillary incisor. The PRIO is nearly 2 cm in diameter and has expanded and eroded the buccal, palatal cortices and eroded the cortex of the floor of the nose. **c, d** are panoramic and transaxial reconstructions, respectively. They display a well-defined unilocular corticated radiolucency in the midline and adjacent to the apex of an incisor, but separated from it by the cysts cortex. It has eroded the palatal cortex entirely. In **d**, the cyst is in communication with the floor of the nose and in **c**. with the nasopalatine or incisive foramen. Acknowledgement: MacDonald [6]

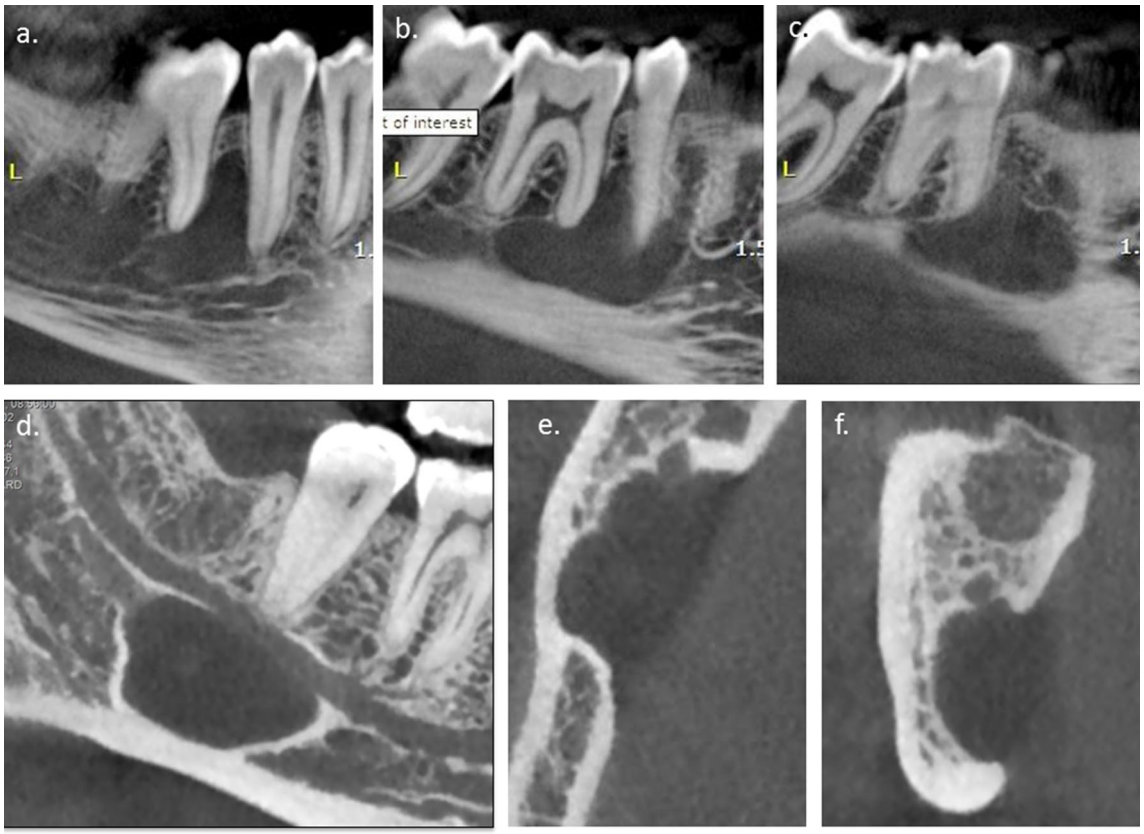

Fig. 19 Cone-beam computed tomographs (CBCT) of a case of a simple bone cyst (SBC) (**a**–**c**) and a lingual bone defect (**d**–**f**). Both are likely to be observed as incidental findings in 1:300 to 1:1000 panoramic radiographs taken in a dental office. **a**–**c** Three buccal-to-lingual panoramic reconstructions, reveal the SBC as a well-defined radiolucency within the mandibular alveolus scalloping up between the roots of the first molar and second premolar teeth. It is also associated with the loss of lamina dura with regards to the mesial root of the first molar and the distal aspect of the second premolar teeth. **d**–**f** are panoramic, axial and transaxial reconstruction, respectively. They reveal the defect reaching to the buccal cortex and up to the mandibular canal. There is a well-defined cortex around the entire periphery of the defect with the exception of a small dehiscence on the inferior aspect of the mandibular canal. Acknowledgement: MacDonald [6]

clearly displayed on panoramic radiographs [11], they still need to be excluded from pulpal necrosis in subjacent teeth, particularly if accompanied by obvious caries, large restoration/s or evidence of dental trauma. A subjacent non-vital tooth would indicate a PRIO. CBCT's cross-sectional imaging would be indicated, where any other lesion is suspected; examples of these are Figs. 3c, d, 5c, d, 7b, 12b, 15c–f.

A PRIO (Fig. 3a, 18a, b) represents at least three separate pathological lesions the radicular cyst, the periapical granuloma and the periapical abscess. Although the granuloma is most likely to regress following optimally performed orthograde endodontics or extraction, this is not necessarily true for the radicular cyst. The latter may account for many of the persistent PRIOs observed in a nearly 30-year-long study of endodontically treated teeth [6, 11, 29].

Compliance with ethical standards

Conflict of interest The author declares that he has no competing interests.

Research involving Human Participants and/or Animals This article does not contain any studies with human or animal subjects performed by any of the authors.

References

1. MacDonald D, Chan A, Harris A, Vertinsky T, Farman AG, Scarfe WC. Diagnosis and management of calcified carotid artery atheroma: dental perspectives. Oral Surg Oral Med Oral Pathol Oral Radiol. 2012;114:533–7.
2. Dagenais M, MacDonald D, Baron M, Hudson M, Tatibouet S, Steele R, Gravel S, Mohit S, El Sayegh T, Pope J, Fontaine A, Masseto A, Matthews D, Sutton E, Thie N, Jones N, Copete M, Kolbinson D, Markland J, Nogueira-Filho G, David Robinson D, Gornitsky M. The Canadian Systemic Sclerosis Oral Health

Study IV: oral radiographic manifestations in systemic sclerosis compared with the general population. Oral Surg Oral Med Oral Pathol Oral Radiol. 2015;120:104–11.
3. MacDonald D, Gu Y, Zhang L, Poh C. Can clinical and radiological features predict recurrence in solitary keratocystic odontogenic tumors? Oral Surg Oral Med Oral Pathol Oral Radiol. 2013;115:263–71.
4. Fujita M, Matsuzaki H, Yanagi Y, Hara M, Katase N, Hisatomi M, Unetsubo T, Konouchi H, Nagatsuka H, Asaumi JI. Diagnostic value of MRI for odontogenic tumours. Dentomaxillofac Radiol. 2013;4:20120265.
5. Lee BD, Lee W, Oh SH, Min SK, Kim EC. A case report of Gardner syndrome with hereditary widespread osteomatous jaw lesions. Oral Surg Oral Med Oral Pathol Oral Radiol Endod. 2009;107:e68–72.
6. MacDonald D. Lesions of the jaws presenting as radiolucencies on cone-beam CT. Clin Radiol. 2016;71:972–85.
7. Horner K, Allen P, Graham J, Jacobs R, Boonen S, Pavitt S, Nackaerts O, Marjanovic E, Adams JE, Karayianni K, Lindh C, van der Stelt P, Devlin H. The relationship between the OSTEODENT index and hip fracture risk assessment using FRAX. Oral Surg Oral Med Oral Pathol Oral Radiol Endod. 2010;110:243–9.
8. MacDonald DS, Li T, Goto TK. A consecutive case series of nevoid basal cell carcinoma syndrome affecting the Hong Kong Chinese. Oral Surg Oral Med Oral Pathol Oral Radiol. 2015;120:396–407.
9. MacDonald DS. A systematic review of the literature of nevoid basal cell carcinoma syndrome affecting East Asians and North Europeans. Oral Surg Oral Med Oral Pathol Oral Radiol. 2015;120:408–15.
10. Papadaki ME, Lietman SA, Levine MA, Olsen BR, Kaban KB, Reichenberger EJ. Cherubism: best clinical practice. Orphanet J Rare Dis. 2012;7(Suppl 1):6. https://doi.org/10.1186/1750-1172-7-S1-S6.
11. MacDonald D. Oral and maxillofacial radiology: a diagnostic approach, 2nd ed. Oxford, United Kingdom: Wiley-Blackwell; 2019 (ISBN 9781119218708).
12. MacDonald DS. Maxillofacial fibro-osseous lesions. Clin Radiol. 2015;70:25–36.
13. MacDonald-Jankowski DS, Yeung R, Li TK, Lee KM. Computed tomography of fibrous dysplasia. Dentomaxillofac Radiol. 2004;33:114–8.
14. Walton K, Grogan TR, Eshaghzadeh E, Hadaya D, Elashoff DA, Aghaloo TL, Tetradis S. Medication related osteonecrosis of the jaw in osteoporotic vs oncologic patients-quantifying radiographic appearance and relationship to clinical findings. Dentomaxillofac Radiol. 2018;28:20180128.
15. Shudo A, Kishimoto H, Takaoka K, Noguchi K. Long-term oral bisphosphonates delay healing after tooth extraction: a single institutional prospective study. Osteoporos Int. 2018;29:2315–21.
16. Soundia A, Hadaya D, Mallya SM, Aghaloo TL, Tetradis S. Radiographic predictors of bone exposure in patients with stage 0 medication-related osteonecrosis of the jaws. Oral Surg Oral Med Oral Pathol Oral Radiol. 2018;126:537–44.
17. MacDonald-Jankowski DS, Wu PC. Cementoblastoma in the Hong Kong Chinese: a report of 4 cases. Oral Surg Oral Med Oral Pathol. 1992;73:760–4.
18. MacDonald-Jankowski DS. Odontomas in a Chinese population. Dentomaxillofac Radiol. 1998;25:186–192.
19. MacDonald-Jankowski DS. Fibro-osseous lesions of the face and jaws. Clin Radiol. 2004;59:11–25.
20. MacDonald-Jankowski DS. Idiopathic osteosclerosis in the jaws of Britons and of the Hong Kong Chinese: radiology and systematic review. Dentomaxillofac Radiol. 1999;28:357–63.
21. Noffke CE, Raubenheimer EJ, MacDonald D. Fibro-osseous disease: harmonizing terminology with biology. Oral Surg Oral Med Oral Pathol Oral Radiol. 2012;114:388–92.
22. MacDonald D, Li T, Leung SF, Curtin J, Yeung A, Martin MA. Extranodal lymphoma arising within the maxillary alveolus: a case report. Oral Surg Oral Med Oral Pathol Oral Radiol. 2017;124:e233-8.
23. MacDonald D, Lim S. Extranodal lymphoma arising within the maxillary alveolus; a systematic review. Oral Radiol. https://doi.org/10.1007/s11282-017-0309-5.
24. Kato H, Kanematsu M, Watanabe H, Kawaguchi S, Mizuta K, Aoki M. Differentiation of extranodal non-Hodgkins lymphoma from squamous cell carcinoma of the maxillary sinus: a multimodality imaging approach. Springerplus. 2015;4:228. https://doi.org/10.1186/s40064-015-0974-y.
25. MacDonald-Jankowski DS, Yeung R, Lee KM, Li TK. Ameloblastoma in the Hong Kong Chinese. Part 2: systematic review and radiological presentation. Dentomaxillofac Radiol. 2004;33:141–51.
26. MacDonald-Jankowski DS, Yeung R, Lee KM, Li TK. Odontogenic myxomas in the Hong Kong Chinese: clinico-radiological presentation and systematic review. Dentomaxillofac Radiol. 2002;31:71–83.
27. MacDonald-Jankowski DS, Yeung RW, Li T, Lee KM. Computed tomography of odontogenic myxoma. Clin Radiol. 2004;59:281–7.
28. Kao YH, Huang IY, Chen CM, Wu CW, Hsu KJ, Chen CM. Late mandibular fracture after lower third molar extraction in a patient with Stafne bone cavity: a case report. J Oral Maxillofac Surg. 2010;68:1698–700.
29. Molven O, Halse A, Fristad I, MacDonald-Jankowski D. Periapical changes following root-canal treatment observed 20–27 years postoperatively. Int Endod J. 2002;35:784–90.